



## Synergistic effect of activated carbon and ultrasonic irradiation on persulfate activation

Jiabing Chen<sup>†</sup>, Ying Wang<sup>†</sup>, Tianyin Huang<sup>\*</sup>, Chengyao Wei

School of Environmental Science and Engineering, Suzhou University of Science and Technology, Suzhou, 215001, China, Tel. +86 0512 68096895; Fax: +86 0512 68096895; email: huangtianyin111@163.com

Received 9 May 2016; Accepted 19 September 2016

### ABSTRACT

Activated carbon (AC) was effective to activate persulfate (PS). Herein, ultrasonic irradiation (US) was introduced into the AC/PS system, and synergistic activation of PS by the combination of US and AC was observed. The effects of various operating parameters on the decolorization of acid orange 7 (AO7), a typical azo dye, by AC/US/PS process were investigated. The results indicated that the decolorization of AO7 gradually increased with increasing AC loading and higher US power. Also, AO7 decolorization efficiency increased with PS/AO7 ratio increasing from 1 to 100, but decreased when the ratio was further increased to 200. pH had little effect on AO7 decolorization, with neutral or slight acidic pHs most suitable for AO7 decolorization. The presence of Cl<sup>-</sup> slightly accelerated AO7 decolorization, and the accelerating effect increased with increasing concentration of Cl<sup>-</sup>. The radical quenching experiments indicated that AO7 decolorization dominantly took place on the surface of AC, and both SO<sub>4</sub><sup>-•</sup> and HO<sup>•</sup> were responsible for AO7 decolorization. The azo band and naphthalene ring of AO7 were destroyed to generate other small intermediate, and finally mineralized to CO<sub>2</sub> and H<sub>2</sub>O.

*Keywords:* Persulfate; Activated carbon; Ultrasonic irradiation; Synergistic activation

### 1. Introduction

Recently, increasing attention has been paid to the sulfate radical (SO<sub>4</sub><sup>-•</sup>) based advanced oxidation process (SR-AOP) owing to its high efficiency for contaminant destruction [1,2]. Persulfate (PS) is the most commonly used oxidant to generate SO<sub>4</sub><sup>-•</sup>. PS is stable at the ambient temperature, but can generate SO<sub>4</sub><sup>-•</sup> after activation by different activators, such as transition metals [3–5], heat [6–8], and ultraviolet radiation [9–11]. Metal ions are the most frequently used activators for PS owing to their low cost and natural abundance. The challenges of its reuse and toxicity, however, limit their wide application [12]. Metal-free carbonaceous material is a promising alternative activator owing to the prevention of metal leaching and secondary contamination to water environment [13,14].

The granular activated carbon (AC) is a common adsorbent in the water treatment owing to its enormous surface

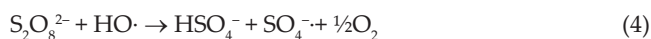
area, porous structure, and characteristic flexibility [15]. Besides its excellent adsorption capacity, AC has been frequently used as a heterogeneous catalyst in the oxidative degradation of contaminants by various oxidants, such as H<sub>2</sub>O<sub>2</sub> [16–18] and O<sub>3</sub> [19]. The combination of AC with other techniques could achieve a much better performance to activate H<sub>2</sub>O<sub>2</sub> to degrade the contaminants in water or wastewater, such as AC/H<sub>2</sub>O<sub>2</sub>/UV and AC/Fenton [20,21]. AC has been recently used to activate PS or peroxymonosulfate (PMS) to generate SO<sub>4</sub><sup>-•</sup>, and destruct different kinds of contaminants [22–25]. The oxygen functional groups on AC surface are potential activators, such as =O, –OH, or –OOH [26]. In comparison with H<sub>2</sub>O<sub>2</sub> or PMS, AC exhibited relatively low efficiency to activate PS. Alternatives to enhance the activation of PS by AC may be to incorporate other technique into the activation system.

Ultrasonic irradiation (US) has been applied to destruct persistent contaminants in aqueous solutions in recent years [27,28]. US is considered as a safer, cleaner technique than UV

\* Corresponding author.

<sup>†</sup> These two authors contributed equally to this work.

and O<sub>3</sub>, and can be operated under ambient conditions [29]. US could induce the formation, growth, and collapse of bubbles in the water. During the collapse of cavitation bubbles, the localized high temperatures and pressures induced the formation of reactive radical species [30]. US could act as an activator for PS to generate SO<sub>4</sub><sup>•-</sup> (Eqs. (1)–(6)), which have been previously applied to degrade various contaminants, such as perfluorooctanoic acid [31], dyes [32], amoxicillin [33], and polycyclic aromatic hydrocarbons (PAHs) [34]. US has also been applied to regenerate AC to desorb and degrade the contaminants [35].



To our best knowledge, activation of PS by the combination of US and AC has not been systematically explored before. Noting that AC is widely used in the conventional water treatment, incorporation of the activated PS process might be highly efficient in the contaminant destruction and AC regeneration. Herein, we investigated the activation of PS by the combination of US and AC to decolorize AO7, a typical azo dye. The purpose of this paper was to: (1) evaluate the synergistic effect of AC and US in the activation of PS; (2) explore the effect of different reaction parameters, such as PS concentration, AC loading, initial pH, US power, and the co-existed ions; and (3) evaluate the product characteristics and the mineralization in the AC/US/PS system.

## 2. Materials and methods

### 2.1. Materials and reagents

The granular AC was purchased from Tianjin Damao Chemical Reagent Company (Tianjin, China), and was ground and sieved through 40–60 mesh before use. Sodium persulfate (Na<sub>2</sub>S<sub>2</sub>O<sub>8</sub>) was purchased from Sigma-Aldrich (St. Louis, MO, USA). Acid orange 7 (AO7; 4-(2-hydroxy-1-naphthylazo)benzenesulfonic acid) was purchased from Sinopharm Chemical Reagent Co., Ltd. (Shanghai, China). Analytical grade methanol (MeOH; CH<sub>3</sub>OH), tert-butyl alcohol (TBA; C<sub>4</sub>H<sub>9</sub>OH), phenol (C<sub>6</sub>H<sub>6</sub>O), sodium hydroxide (NaOH), sulfuric acid (H<sub>2</sub>SO<sub>4</sub>), and sodium chloride (NaCl) were obtained from Shanghai Chemical Reagent Company (Shanghai, China). Deionized (DI) water was produced using a Millipore Milli-Q Ultrapure Gradient A10 purification system.

### 2.2. Experimental procedure

The degradation of AO7 was conducted in a 250-mL clear glass flasks located in an ultrasound clean bath operating

at 40 kHz with an actual power of 9.8 W/cm<sup>2</sup>. Typically, AC was added to the reactor containing 250 mL solution of AO7 and PS at an initial pH 7, and then continuously stirred with mechanistic stirring. At the pre-determined time, 5 mL of sample was withdrawn and quenched with excess NaNO<sub>2</sub> immediately. Afterward, the quenched sample was filtered through 0.45 μm membrane, and the concentration was measured on a UV-Vis spectrophotometers. In the experiments investigating the impact of solution pH, NaOH or H<sub>2</sub>SO<sub>4</sub> was used to adjust the solution pH. All the experiments were carried out in duplicate or more.

### 2.3. Analysis

The absorbance of AO7 at 484 nm was monitored on a UV-Vis spectrophotometer (Mapada UV-1600). A calibration curve was established between the concentration (*y*) and absorbance (*x*) of AO7, i.e.,  $y = 16.507 \times x - 0.2026$  ( $R^2 = 0.9999$ ). Hence, the concentration could be calculated from the calibration curve after the measurement of the absorbance. The UV-Vis spectra scan between 200 and 600 nm was also performed in this spectrophotometer. Total organic carbon (TOC) was analyzed with a TOC-LCPH, and the detection limit was 0.01 mg/L.

The degradation products of AO7 were determined by gas chromatography-mass spectrometry (GC-MS; Agilent 7890A/5975C). NaCl (1 g) was added to 5 ml of sample, and the pH was adjusted to 2 using H<sub>2</sub>SO<sub>4</sub>. Then the solution was extracted with 30 ml of CH<sub>2</sub>Cl<sub>2</sub> for 3 times (10 ml × 3). The extract was dehydrated with Na<sub>2</sub>SO<sub>4</sub>, and then evaporated in a rotary evaporator at 40°C to final volume of 1 ml. The products were analyzed on GC-MS equipped with HP-5MS (30 m × 0.25 mm × 0.25 μm). Injection was performed in the splitless mode at an injection temperature of 250°C and with an injection volume of 1 μL. The carrier gas was helium at a constant velocity of 1 ml/min. The initial oven temperature was set at 40°C for 2 min, and then increased to 100°C at the rate of 12°C/min. After this, it was subsequently increased to 200°C at 5°C/min, and then temperature was raised at 20°C/min and for 10 min and kept at 270°C. Mass spectra were obtained in electron impact ionization (EI) mode with electron energy 70 eV.

## 3. Results and discussion

### 3.1. Decolorization of AO7 under different systems

The preliminary experiments were performed to investigate AO7 decolorization under different systems, and the results were shown in Fig. 1. As shown in Fig. 1(A), PS alone exhibited negligible effect on AO7 decolorization, suggesting that PS was not activated at the ambient temperature. AC alone decolorized 27.5% of AO7 after 30 min, owing to adsorption. The combination of PS and AC induced higher decolorization of AO7 after 30 min than that with PS or AC alone, indicating the ability of AC to activate PS to decolorize AO7 [22]. The introduction of US in the system containing AC or AC/PS could significantly increase AO7 decolorization. To be specific, AO7 decolorization increased to 81.6% after 30 min in the US/AC system, while almost complete decolorization of AO7 was observed within 25 min in the AC/PS/US system, which was much faster than that in other systems. The decolorization

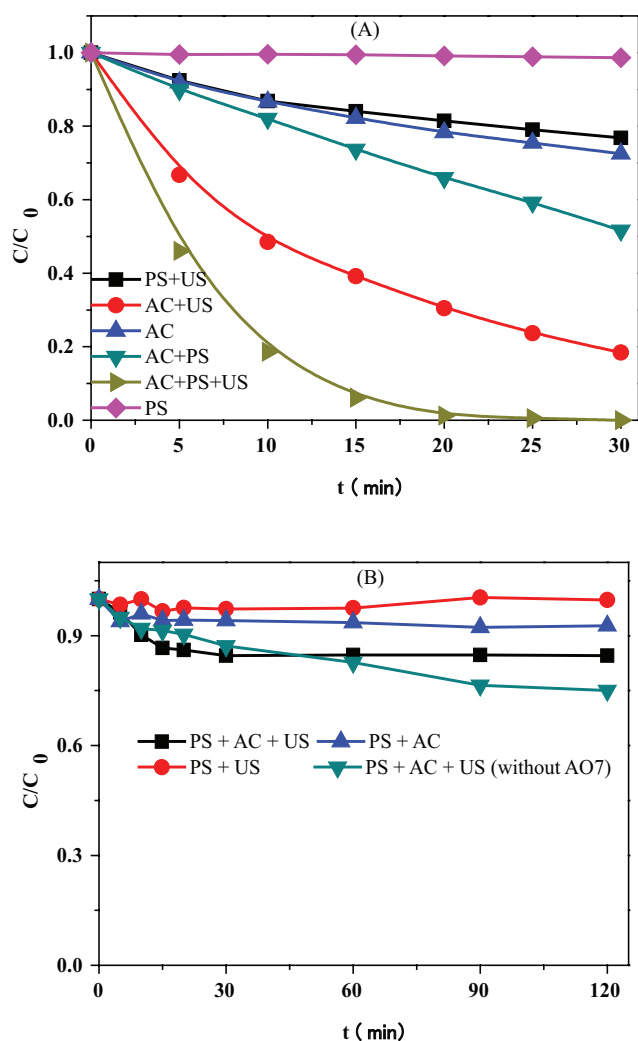


Fig. 1. Decolorization of AO7 (A) and decomposition of PS (B) under different systems: PS/AO7 molar ratio = 60/1, AC loading = 0.8 g/L, AO7 = 0.057 mM.

of AO7 in AC/PS, US/PS, and AC/US/PS systems well conformed to the pseudo-first-order kinetics, and the apparent first-order rate constants were calculated to be 0.083, 0.0217, and 0.216  $\text{min}^{-1}$  in the AC/PS, US/PS, and AC/US/PS systems, respectively. Rate constant in the AC/US/PS system was much larger than the sum of the constant in AC/PS and US/PS system. Therefore, synergistic activation of PS was observed by the combination of US and AC. After introduction of US, US was able to activate PS to decolorize AO7. More importantly, AC was dispersed to smaller particles, and the surface area became larger (Brunauer Emmett-Teller (BET) surface area increased from 381 to 480  $\text{m}^2/\text{g}$ ), which was favorable for the adsorption of AO7 on AC. On the other hand, smaller AC particle could render more active sites for PS activation (as shown in Fig. 1(A)).

We further monitored the decomposition of PS under different systems. As shown in Fig. 1(B), only slight decomposition of PS was observed after introduction of AC or US into the PS solution, indicating the low efficiency of AC or US in PS activation. When AC and US were simultaneously introduced in

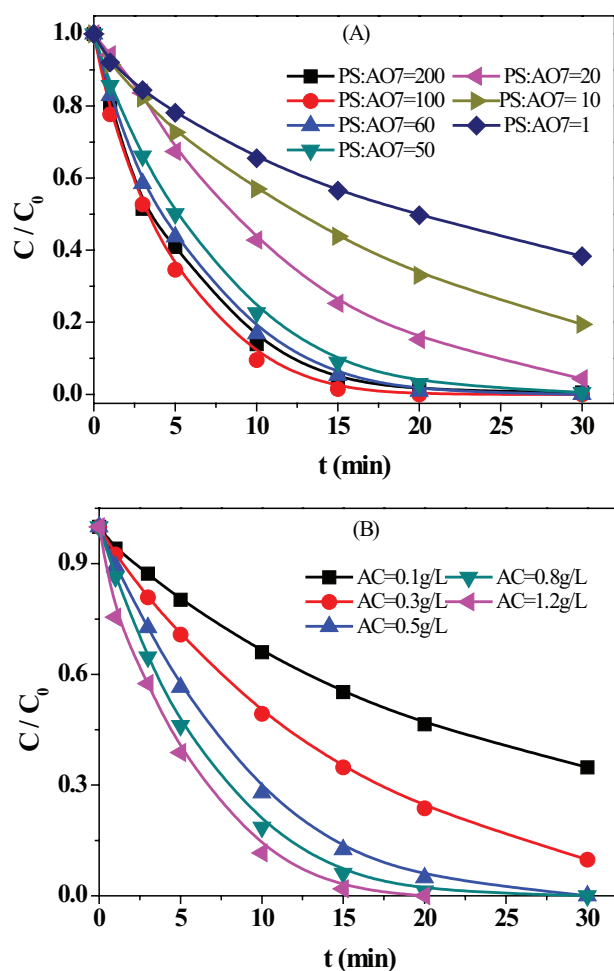


Fig. 2. Effect of PS concentration (A) and AC loading (B) on the decolorization of AO7 in the AC/US/PS system: AO7 = 0.057 mM, (A) AC loading = 0.8 g/L, (B) PS/AO7 molar ratio = 60/1.

the PS solution, significant decomposition of PS was observed in the initial 30 min. Afterward, the decomposition slowed down and finally ceased. The decomposition trend of PS was identical to that of AO7 decolorization, implying that AO7 decolorization was induced by the oxidative species generated from PS decomposition. We further investigated PS decomposition in the AC/US/PS system in the absence of AO7. Significant decomposition was still observed in the system without AO7, and the decomposition trend was different from that with AO7. For example, the cease of PS decomposition was not observed along the 120 min reaction. This phenomenon might be explained by the occupation of active sites of AC by the degradation products of AO7, unfavorable for further activation of PS.

### 3.2. Effect of PS concentration

The effect of PS concentration on AO7 decolorization was investigated with PS/AO7 molar ratios ranging from 1:1 to 200:1, and the results were depicted in Fig. 2(A). The decolorization efficiency of AO7 was gradually increased with increasing PS/AO7 ratio from 1 to 100. To be specific, AO7 decolorization efficiency increased from 61.7% to 100% after 30 min when the PS/AO7 ratio increased from 1 to 50.

Complete decolorization was achieved within 20 min when the ratio further increased to 100. However, further increase of the ratio to 200 slightly retarded AO7 decolorization. Although higher concentration of PS could generate more  $\text{SO}_4^{\cdot-}$ , excess PS could quench the radicals (Eqs. (7) and (8)), thus unfavorable for the dye decolorization. This result was consistent with the degradation of perfluorooctanoic acid in the activated PS system [36].



### 3.3. Effect of AC loading

Effect of AC loadings on AO7 decolorization was shown in Fig. 2(B). AO7 decolorization increased with increasing loadings of AC. For example, the decolorization of AO7 increased from 65.2% to 90.1% after 30 min when the AC loading raising from 0.1 to 0.3 g/L. Afterward, complete decolorization was observed after 30 min when AC loading further increased to 0.5 g/L, and even after 20 min at AC loading of 1.2 g/L. Higher loading of AC could supply more reactive sites for PS activation; thus, more radicals were generated to decolorize AO7.

### 3.4. Effect of initial pH

Effect of pH on AO7 decolorization in the AC/US/PS system was also investigated, and the result was demonstrated in Fig. 3. As shown in Fig. 3(A), pH had a little effect on AO7 decolorization. Generally, neutral or slight acidic pHs were favorable for AO7 decolorization, while acidic or alkaline pHs slightly retarded the decolorization of AO7. At acidic pHs, the surface of AC is positively charged ( $\text{pH}_{\text{pzc}} = 8.4$ ), while the dye molecule is always negatively charged in the investigated pHs. Hence, lower pHs were beneficial for the adsorption of AO7 on AC (Fig. 3(B)). AO7 could compete with PS for the active site on the surface of AC. Thus, more AO7 adsorption on AC could cause the reduction of PS adsorption on AC, which was unfavorable for the activation of PS on the surface of AC, and the decolorization of AO7. At alkaline pH, the surface of AC carries negative charges, thus unbeneficial for the adsorption of PS anion. Therefore, alkaline pH also unfavored PS activation in the AC/US/PS system. Moreover, under alkaline pH,  $\text{SO}_4^{\cdot-}$  could be scavenged by the hydroxyl ions according to the Eq. (9), thus reduced the decolorization of AO7 as well.



### 3.5. Effect of the US power

The power of US is a very important factor for US engineering design [33,37]. Effect of US power on the decolorization of AO7 in the US/AC/PS system was investigated. As shown in Fig. 4(A), without US irritation, only slight decolorization of AO7 was observed, with 48.3% remained

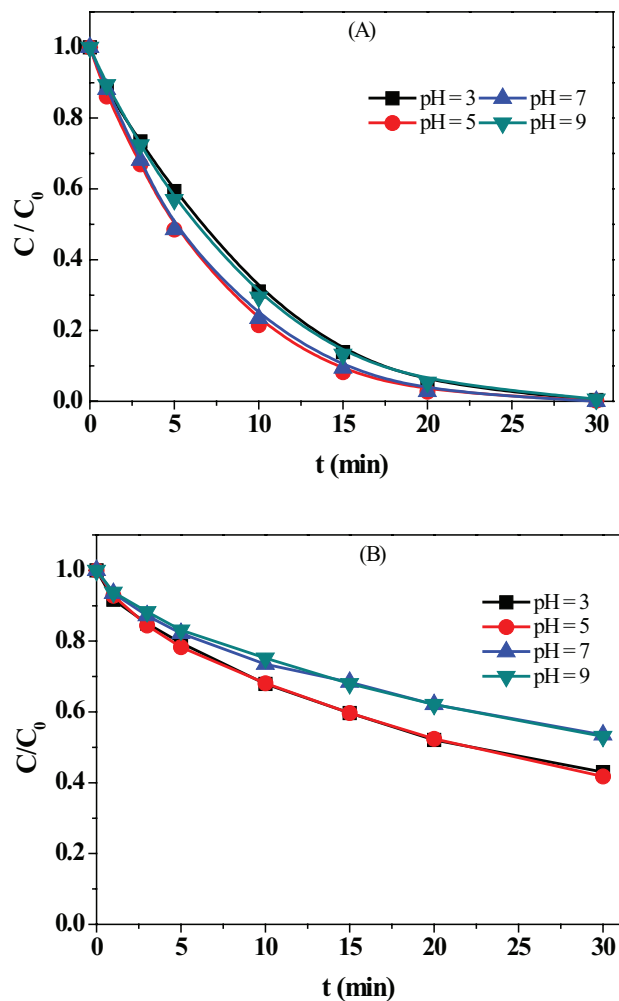


Fig. 3. Effect of initial pH on AO7 decolorization in the AC/PS/US system (A) and AC/US system (B); PS/AO7 molar ratio = 60/1, AC loading = 0.8 g/L, AO7 = 0.057 mM.

after 30 min in the solution. After introduction of US, AO7 decolorization significantly increased. In addition, the decolorization efficiency increased with increasing US power. For example, about 80% decolorization of AO7 was achieved after 30 min when  $3.9 \text{ W/cm}^2$  of US power was introduced. Almost complete decolorization was observed after 20 and 30 min for  $5.9$  and  $9.8 \text{ W/cm}^2$  of US power, respectively. Higher US power means that more cavities could be generated, thus increasing the cumulative pressure pulse and the number of free radicals in the systems [32,37]. Also, the increase of US power could reduce the lifetime of the bubble, thus enhance the opportunity of free radicals to escape from the bubble and migrate toward the liquid bulk before the recombination between each other [38].

### 3.6. Effect of chloride ion

Because there is a potential risk of adsorbable organic halogen (AOX) formation, the presence of chloride ion is not desired in AOPs. However, NaCl is widely used in the dyeing industry to accelerate the dyeing process; hence,

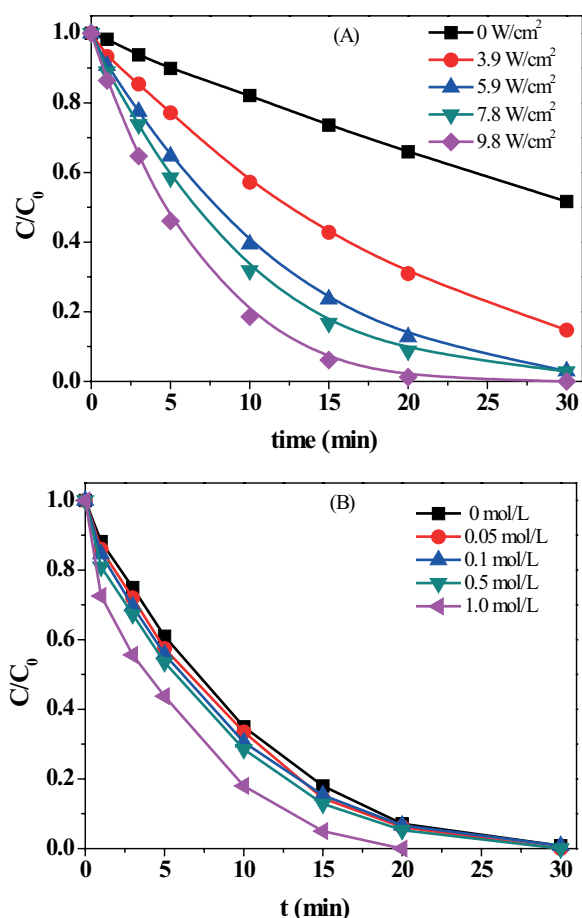


Fig. 4. Effect of the US power (A) and NaCl concentration (B) on AO7 decolorization in the AC/US/PS system: PS/AO7 molar ratio = 60:1, AC loading = 0.8 g/L, AO7 = 0.057 mM.

dyes wastewater is always characterized by highly concentrated NaCl (5–60 g/L) [39]. Therefore, effect of Cl<sup>-</sup> on AO7 decolorization was also explored in this work. As shown in Fig. 4(B), decolorization of AO7 was slightly affected after the addition of different concentration of Cl<sup>-</sup>. Generally, AO7 decolorization increased with the increasing concentration of Cl<sup>-</sup>. In the presence of Cl<sup>-</sup>, Cl<sup>-</sup> could be reactive with SO<sub>4</sub><sup>-•</sup> to generate other chloride radical species (Eqs. (10)–(15)) [40–42]. All these reactions were a major sink for SO<sub>4</sub><sup>-•</sup>, which affected the degradation of contaminants. The generated Cl<sub>2</sub> or HOCl was reported to be an excellent bleaching agent for azo dyes [42]; hence, higher concentration of Cl<sup>-</sup> in the system could induce more generation of HOCl, thus improving the decolorization of AO7.

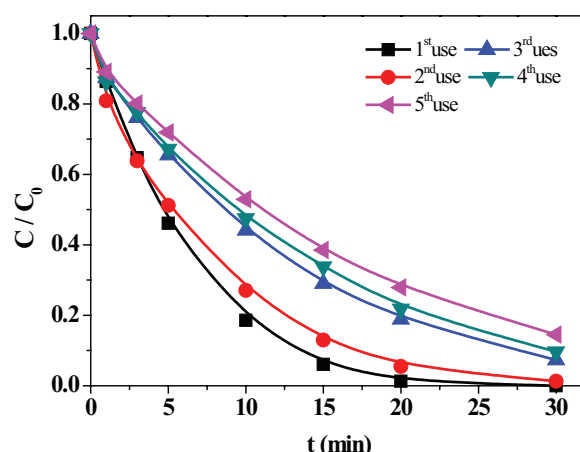


Fig. 5. The reusability of AC in the AC/US/PS system: PS/AO7 = 60/1, AC loading = 0.8 g/L, AO7 = 0.057 mM.



### 3.7. Reuse of AC

Sequential experiments were carried out to investigate the reusability of AC in the activation of PS under US irradiation. As shown in Fig. 5, the decolorization of AO7 slightly decreased in the second run, and almost complete decolorization was still observed after 30 min. A significant decrease of the decolorization was observed in the third run. Afterward, AC exhibited slight deactivation in the following runs, and 85% decolorization efficiency could be still achieved in the fifth run. During the reaction, the anion ions (e.g., S<sub>2</sub>O<sub>8</sub><sup>2-</sup> and SO<sub>4</sub><sup>2-</sup>) and degradation intermediate of AO7 might be adsorbed on the surface of AC, thus decreased the activation sites on AC for PS. In addition, AC could be dispersed to small particles under US irradiation, which might escape from the membrane filtration during the separation.

### 3.8. Radical mechanism

Both of SO<sub>4</sub><sup>-•</sup> and HO<sup>•</sup> are common reactive radical species responsible for contaminant degradation in the activated PS process. Alcohols with alpha hydrogen are moderately reactive with both SO<sub>4</sub><sup>-•</sup> and HO<sup>•</sup>, such as MeOH (reaction rate constants of 9.7 × 10<sup>8</sup> and 3.2 × 10<sup>6</sup> M<sup>-1</sup> s<sup>-1</sup> for HO<sup>•</sup> and SO<sub>4</sub><sup>-•</sup>, respectively). On the other hand, alcohols without alpha hydrogen, e.g., TBA, react with HO<sup>•</sup> approximately thousandfold faster than SO<sub>4</sub><sup>-•</sup> ((3.8–7.6) × 10<sup>8</sup> and (4–9.1) × 10<sup>5</sup> M<sup>-1</sup> s<sup>-1</sup> for HO<sup>•</sup> and SO<sub>4</sub><sup>-•</sup>, respectively) [43]. Thus, MeOH and TBA are always selected as the probes to differentiate the contribution of the radical species for contaminant degradation. As shown in Fig. 6, MeOH and TBA indeed slightly inhibited AO7 decolorization, and the inhibition slightly increased with the increase of their concentration. Because MeOH and TBA are hydrophilic chemicals, they are assumed

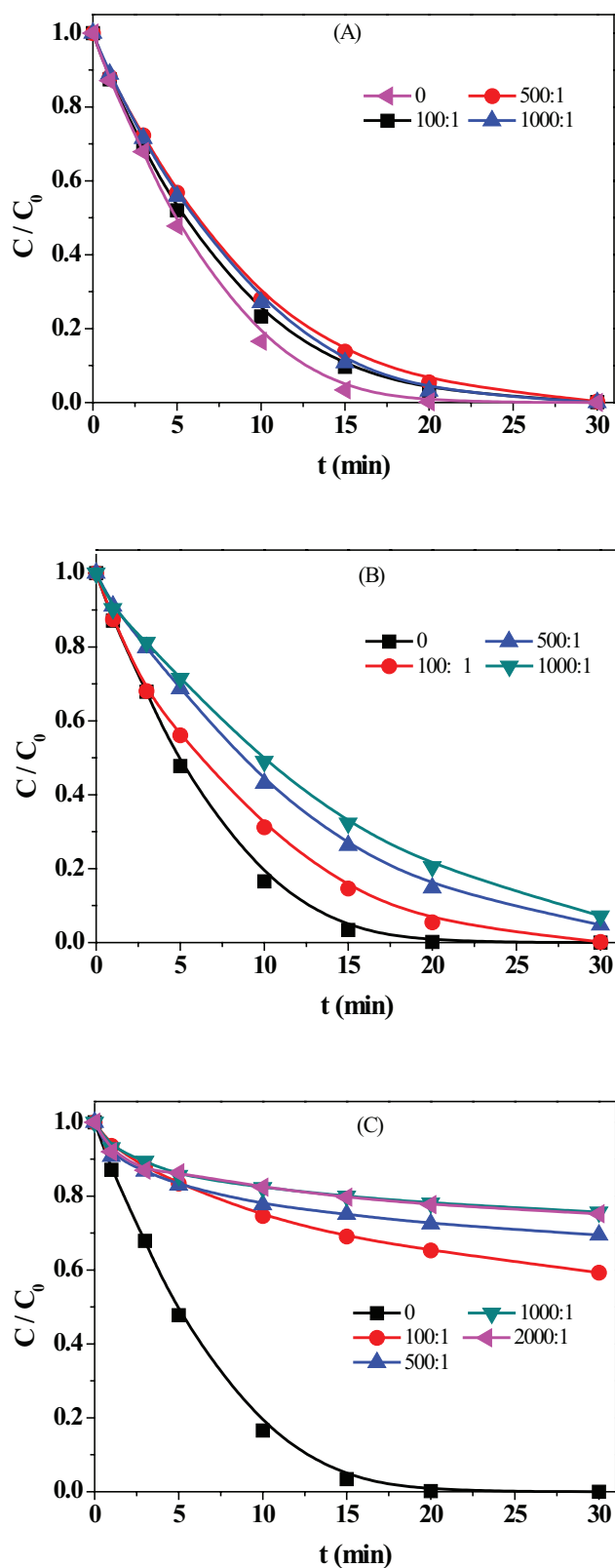


Fig. 6. Decolorization of AO7 in the presence of different concentration of MeOH (A), TBA (B), and phenol (C): PS/AO7 = 60/L, AC loading = 0.8 g/L, AO7 = 0.057 mM, different concentration of radical scavengers at scavenger/AO7 molar ratio = 100/1, 500/1, 1,000/1.

to be difficult to accumulate on the surface of AC. The dielectric constant of TBA is smaller than that of MeOH [44]; thus, TBA is relatively easier to close to the surface of AC. Therefore, from the results of MeOH and TBA, we could preliminarily conclude that the radical-induced decolorization of AO7 did not take place in the bulk solution, and most likely on the surface of AC.

To further confirm the radical reactions on AC surface, we investigated the effect of phenol on the decolorization of AO7 in our reaction system. Phenol, another strong scavenger for  $\text{SO}_4^{\cdot-}$  and  $\text{HO}\cdot$  ( $6.6 \times 10^9$  and  $8.8 \times 10^9 \text{ M}^{-1} \text{ s}^{-1}$  for  $\text{SO}_4^{\cdot-}$  and  $\text{HO}\cdot$ , respectively), was frequently used to explore the radical species in the heterogeneously activated PS process [22]. As shown in Fig. 6(C), phenol exhibited a remarkable inhibition effect on AO7 decolorization. For example, when phenol/AO7 ratio of 100 was added into the solution, the decolorization of AO7 decreased from 100% to 40% after 30 min. When the ratio increased to 1,000, the decolorization of AO7 was almost identical to AC adsorption when PS was not added. Thus, the oxidative degradation of AO7 was almost completely ceased. Compared with MeOH and TBA, phenol is relatively hydrophobic; thus, it is much easier to approach to the surface of AC. It could strongly compete with AO7 for the radical species on the surface of AC. From the above results, we could propose that AO7 decolorization occurred on the surface of AC rather than the bulk solution, and both  $\text{SO}_4^{\cdot-}$  and  $\text{HO}\cdot$  were responsible for the decolorization of AO7, which was consistent with the previous result in the heterogeneously activated PS process [22,44].

### 3.9. Degradation products and mineralization analysis

The UV-Vis spectra of AO7 were monitored during the decolorization in the US/AC/PS system. As shown in Fig. 7(A), three peaks at 310, 430, and 484 nm were observed in the spectrum of AO7, which reflects the naphthalene, hydrazone, and azo structure, respectively [45,46]. During the reaction, the intensity of the three peaks gradually decreased as the reaction proceeded, and finally disappeared after 30 min reaction. This result indicated that AO7 was completely decolorized, i.e., the azo bond was destroyed and the naphthalene ring was destructed to other small molecules, and even mineralized to  $\text{CO}_2$  and  $\text{H}_2\text{O}$ . We further identified the products of AO7 by GC-MS, and the proposed structures were shown in Fig. 8. Six main products were identified during the degradation of AO7. All these products have been previously reported [39,47–49]. AO7 was supposed to be oxidized to naphthalene-type compounds (e.g., 1,2-naphthoquinone, coumarin, and 1-nitro-2-naphthalenol) after the cleavage of azo band. These products were subsequently oxidized to generate fused heterocyclic compounds (e.g., phthalic anhydride) and other smaller molecular products (e.g., phenol and phthalic acid), and finally mineralized to  $\text{CO}_2$  and  $\text{H}_2\text{O}$ .

To further verify the mineralization of AO7, we monitored the variation of TOC during the reaction. As shown in Fig. 7(B), significant removal of TOC was observed after 60 min in the US/AC/PS system. However, such

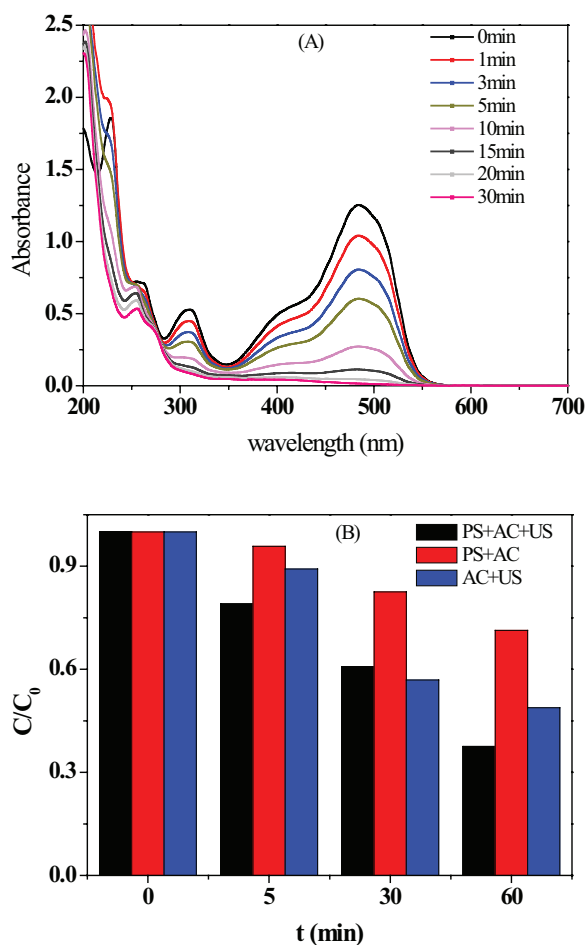


Fig. 7. UV-Vis spectra (A) and TOC abatement (B) during AO7 decolorization: PS/AO7 molar ratio = 60:1, AC loading = 0.8 g/L, AO7 = 0.057 mM, TOC<sub>0</sub> = 10.86 mg/L.

high removal efficiency of TOC could not be completely attributed to the mineralization. Because TOC removal was also observed in the US/AC system, which could be ascribed to the adsorption on AC. Compared with the adsorption of TOC on AC, TOC removal in the US/AC/PS was higher. Therefore, the mineralization of AO7 also significantly contributed to the TOC removal. TOC removal in the AC/PS system was much lower than that in the AC/US and AC/US/PS system, indicating lower mineralization of AO7 by AC activated PS. Therefore, the synergistic activation of PS by US and AC exhibited a much higher decolorization and mineralization capacity in the degradation of azo dye.

#### 4. Conclusions

Synergistic effect of AC and US was observed in activating PS to decolorization of AO7. Decolorization efficiency of AO7 increased with PS/AO7 ratio increasing from 1 to 100, but decreased when the ratio further increased to 200. Higher loading of AC, raising US power, and elevating Cl<sup>-</sup> concentration were favorable for AO7 decolorization. Both SO<sub>4</sub><sup>-</sup> and HO<sup>•</sup> were responsible

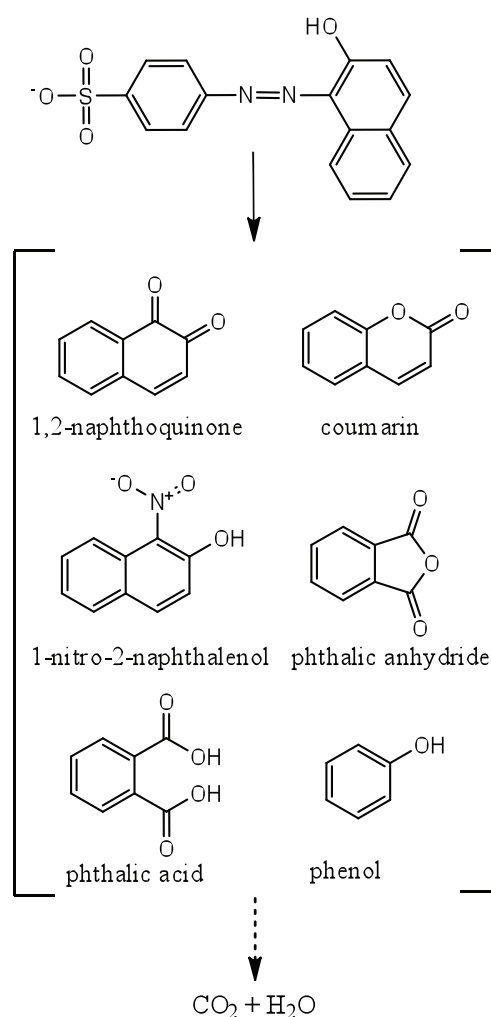


Fig. 8. Degradation products analysis by GC-MS.

for AO7 decolorization, which mainly took place on the surface of AC. The azo band and naphthalene ring was destructed to other small molecules, and even mineralized to CO<sub>2</sub> and H<sub>2</sub>O.

#### Acknowledgement

We sincerely thank the National Natural Science Foundation of China (51478283, 51509175), Suzhou Key Lab of Separation and Purification Materials & Technologies (SZS201512), and Preponderant Discipline Construction Project in higher education of Jiangsu Province, China for financially supporting this work.

#### References

- [1] A. Rastogi, S.R. Al-Abed, D.D. Dionysiou, Effect of inorganic, synthetic and naturally occurring chelating agents on Fe(II) mediated advanced oxidation of chlorophenols, *Water Res.*, 43 (2009) 684–694.
- [2] G.P. Anipsitakis, D.D. Dionysiou, Degradation of organic contaminants in water with sulfate radicals generated by the conjunction of peroxymonosulfate with cobalt, *Environ. Sci. Technol.*, 37 (2003) 4790–4797.

- [3] G.P. Anipsitakis, D.D. Dionysiou, Radical generation by the interaction of transition metals with common oxidants, *Environ. Sci. Technol.*, 38 (2004) 3705–3712.
- [4] X. Xiong, B. Sun, J. Zhang, N. Gao, J. Shen, J. Li, X. Guan, Activating persulfate by Fe<sup>0</sup> coupling with weak magnetic field: performance and mechanism, *Water Res.*, 62 (2014) 53–62.
- [5] Y. Ren, L. Lin, J. Ma, J. Yang, J. Feng, Z. Fan, Sulfate radicals induced from peroxymonosulfate by magnetic ferrosphalite MFe<sub>2</sub>O<sub>4</sub> (M = Co, Cu, Mn, and Zn) as heterogeneous catalysts in the water, *Appl. Catal., B*, 165 (2015) 572–578.
- [6] M. Nie, Y. Yang, Z. Zhang, C. Yan, X. Wang, H. Li, W. Dong, Degradation of chloramphenicol by thermally activated persulfate in aqueous solution, *Chem. Eng. J.*, 246 (2014) 373–382.
- [7] A. Ghauch, A.M. Tuqan, N. Kibbi, Ibuprofen removal by heated persulfate in aqueous solution: a kinetics study, *Chem. Eng. J.*, 197 (2012) 483–492.
- [8] J. Deng, Y. Shao, N. Gao, Y. Deng, S. Zhou, X. Hu, Thermally activated persulfate (TAP) oxidation of antiepileptic drug carbamazepine in water, *Chem. Eng. J.*, 228 (2013) 765–771.
- [9] T.K. Lau, W. Chu, N.J.D. Graham, The aqueous degradation of butylated hydroxyanisole by UV/S<sub>2</sub>O<sub>8</sub><sup>2-</sup>: study of reaction mechanisms via dimerization and mineralization, *Environ. Sci. Technol.*, 41 (2006) 613–619.
- [10] Y. Qian, X. Guo, Y. Zhang, Y. Peng, P. Sun, C.H. Huang, J. Niu, X. Zhou, J.C. Crittenden, Perfluorooctanoic acid degradation using UV–persulfate process: modeling of the degradation and chlorate formation, *Environ. Sci. Technol.*, 50 (2016) 772–781.
- [11] C.W. Wang, C. Liang, Oxidative degradation of TMAH solution with UV persulfate activation, *Chem. Eng. J.*, 254 (2014) 472–478.
- [12] P.R. Shukla, S.B. Wang, H.Q. Sun, H.M. Ang, M. Tade, Activated carbon supported cobalt catalysts for advanced oxidation of organic contaminants in aqueous solution, *Appl. Catal., B*, 100 (2010) 529–534.
- [13] H. Sun, C. Kwan, A. Suvorova, H.M. Ang, M.O. Tade, S. Wang, Catalytic oxidation of organic pollutants on pristine and surface nitrogen-modified carbon nanotubes with sulfate radicals, *Appl. Catal., B*, 154–155 (2014) 134–141.
- [14] H. Lee, H.J. Lee, J. Jeong, J. Lee, N.B. Park, C. Lee, Activation of persulfates by carbon nanotubes: oxidation of organic compounds by nonradical mechanism, *Chem. Eng. J.*, 266 (2015) 28–33.
- [15] G. Mezohegyi, F.P. van der Zee, J. Font, A. Fortuny, A. Fabregat, Towards advanced aqueous dye removal processes: a short review on the versatile role of activated carbon, *J. Environ. Manage.*, 102 (2012) 148–164.
- [16] T.A. Kurniawan, W.H. Lo, Removal of refractory compounds from stabilized landfill leachate using an integrated H<sub>2</sub>O<sub>2</sub> oxidation and granular activated carbon (GAC) adsorption treatment, *Water Res.*, 43 (2009) 4079–4091.
- [17] S.G. Huling, P.K. Jones, T.R. Lee, Iron optimization for Fenton-driven oxidation of MTBE-spent granular activated carbon, *Environ. Sci. Technol.*, 41 (2007) 4090–4096.
- [18] A. Dhaouadi, N. Adhoum, Heterogeneous catalytic wet peroxide oxidation of paraquat in the presence of modified activated carbon, *Appl. Catal., B*, 97 (2010) 227–235.
- [19] P.C.C. Faria, J.J.M. Orfao, M.F.R. Pereira, Activated carbon and ceria catalysts applied to the catalytic ozonation of dyes and textile effluents, *Appl. Catal., B*, 88 (2009) 341–350.
- [20] N.H. Ince, I.G. Apikyan, Combination of activated carbon adsorption with light-enhanced chemical oxidation via hydrogen peroxide, *Water Res.*, 34 (2000) 4169–4176.
- [21] R.S. Hornig, I.C. Tseng, Regeneration of granular activated carbon saturated with acetone and isopropyl alcohol via a recirculation process under H<sub>2</sub>O<sub>2</sub>/UV oxidation, *J. Hazard. Mater.*, 154 (2008) 366–372.
- [22] S. Yang, X. Yang, X. Shao, R. Niu, L. Wang, Activated carbon catalyzed persulfate oxidation of Azo dye acid orange 7 at ambient temperature, *J. Hazard. Mater.*, 186 (2011) 659–666.
- [23] S.G. Huling, S. Ko, S. Park, E. Kan, Persulfate oxidation of MTBE- and chloroform-spent granular activated carbon, *J. Hazard. Mater.*, 192 (2011) 1484–1490.
- [24] Y.C. Lee, S.L. Lo, J. Kuo, C.P. Huang, Promoted degradation of perfluorooctanoic acid by persulfate when adding activated carbon, *J. Hazard. Mater.*, 261 (2013) 463–469.
- [25] J. Zhang, X.T. Shao, C. Shi, S.Y. Yang, Decolorization of Acid Orange 7 with peroxymonosulfate oxidation catalyzed by granular activated carbon, *Chem. Eng. J.*, 232 (2013) 259–265.
- [26] C. Liang, Y.T. Lin, W.H. Shih, Treatment of trichloroethylene by adsorption and persulfate oxidation in batch studies, *Ind. Eng. Chem. Res.*, 48 (2009) 8373–8380.
- [27] Y. Nagata, M. Nakagawa, H. Okuno, Y. Mizukoshi, B. Yim, Y. Maeda, Sonochemical degradation of chlorophenols in water, *Ultrason. Sonochem.*, 7 (2000) 115–120.
- [28] N.N. Mahamuni, A.B. Pandit, Effect of additives on ultrasonic degradation of phenol, *Ultrason. Sonochem.*, 13 (2006) 165–174.
- [29] B. Li, L. Li, K. Lin, W. Zhang, S. Lu, Q. Luo, Removal of 1,1,1-trichloroethane from aqueous solution by a sono-activated persulfate process, *Ultrason. Sonochem.*, 20 (2013) 855–863.
- [30] C. Cai, L. Wang, H. Gao, L. Hou, H. Zhang, Ultrasound enhanced heterogeneous activation of peroxydisulfate by bimetallic Fe-Co/GAC catalyst for the degradation of Acid Orange 7 in water, *J. Environ. Sci.*, 26 (2014) 1267–1273.
- [31] J.C. Lin, S.L. Lo, C.Y. Hu, Y.C. Lee, J. Kuo, Enhanced sonochemical degradation of perfluorooctanoic acid by sulfate ions, *Ultrason. Sonochem.*, 22 (2015) 542–547.
- [32] P. Gayathri, R.P.J. Dorathi, K. Palanivelu, Sonochemical degradation of textile dyes in aqueous solution using sulphate radicals activated by immobilized cobalt ions, *Ultrason. Sonochem.*, 17 (2010) 566–571.
- [33] S. Su, W. Guo, C. Yi, Y. Leng, Z. Ma, Degradation of amoxicillin in aqueous solution using sulphate radicals under ultrasound irradiation, *Ultrason. Sonochem.*, 19 (2012) 469–474.
- [34] D. Deng, X. Lin, J. Ou, Z. Wang, S. Li, M. Deng, Y. Shu, Efficient chemical oxidation of high levels of soil-sorbed phenanthrene by ultrasound induced, thermally activated persulfate, *Chem. Eng. J.*, 265 (2015) 176–183.
- [35] J.L. Lim, M. Okada, Regeneration of granular activated carbon using ultrasound, *Ultrason. Sonochem.*, 12 (2005) 277–282.
- [36] Y.C. Lee, S.L. Lo, J. Kuo, Y.L. Lin, Persulfate oxidation of perfluorooctanoic acid under the temperatures of 20–40 °C, *Chem. Eng. J.*, 198–199 (2012) 27–32.
- [37] W.S. Chen, Y.C. Su, Removal of dinitrotoluenes in wastewater by sono-activated persulfate, *Ultrason. Sonochem.*, 19 (2012) 921–927.
- [38] C. Pétrier, A. Francony, Ultrasonic waste-water treatment: incidence of ultrasonic frequency on the rate of phenol and carbon tetrachloride degradation, *Ultrason. Sonochem.*, 4 (1997) 295–300.
- [39] R. Yuan, S.N. Ramjaun, Z. Wang, J. Liu, Photocatalytic degradation and chlorination of azo dye in saline wastewater: kinetics and AOX formation, *Chem. Eng. J.*, 192 (2012) 171–178.
- [40] K.H. Chan, W. Chu, Degradation of atrazine by cobalt-mediated activation of peroxymonosulfate: different cobalt counteranions in homogeneous process and cobalt oxide catalysts in photolytic heterogeneous process, *Water Res.*, 43 (2009) 2513–2521.
- [41] J. Chen, Y. Qian, H. Liu, T. Huang, Oxidative degradation of diclofenac by thermally activated persulfate: implication for ISCO, *Environ. Sci. Pollut. Res.*, 23 (2016) 3824–3833.
- [42] X.Y. Lou, Y.G. Guo, D.X. Xiao, Z.H. Wang, S.Y. Lu, J.S. Liu, Rapid dye degradation with reactive oxidants generated by chloride-induced peroxymonosulfate activation, *Environ. Sci. Pollut. Res.*, 20 (2013) 6317–6323.
- [43] J.C. Yan, M. Lei, L.H. Zhu, M.N. Anjum, J. Zou, H.Q. Tang, Degradation of sulfamonomethoxine with Fe<sub>3</sub>O<sub>4</sub> magnetic nanoparticles as heterogeneous activator of persulfate, *J. Hazard. Mater.*, 186 (2011) 1398–1404.
- [44] H.Y. Liang, Y.Q. Zhang, S.B. Huang, I. Hussain, Oxidative degradation of p-chloroaniline by copper oxidate activated persulfate, *Chem. Eng. J.*, 218 (2013) 384–391.
- [45] C. Bauer, P. Jacques, A. Kalt, Photooxidation of an azo dye induced by visible light incident on the surface of TiO<sub>2</sub>, *J. Photochem. Photobiol., A*, 140 (2001) 87–92.
- [46] W. Feng, D. Nansheng, H. Helin, Degradation mechanism of azo dye C.I. reactive red 2 by iron powder reduction and

- photooxidation in aqueous solutions, *Chemosphere*, 41 (2000) 1233–1238.
- [47] R. Yuan, S.N. Ramjaun, Z. Wang, J. Liu, Effects of chloride ion on degradation of Acid Orange 7 by sulfate radical-based advanced oxidation process: implications for formation of chlorinated aromatic compounds, *J. Hazard. Mater.*, 196 (2011) 173–179.
- [48] H.Z. Zhao, Y. Sun, L.N. Xu, J.R. Ni, Removal of Acid Orange 7 in simulated wastewater using a three-dimensional electrode reactor: removal mechanisms and dye degradation pathway, *Chemosphere*, 78 (2010) 46–51.
- [49] J. Wu, H. Zhang, J. Qiu, Degradation of Acid Orange 7 in aqueous solution by a novel electro/Fe<sup>2+</sup>/peroxydisulfate process, *J. Hazard. Mater.*, 215 (2012) 138–145.